RESEARCH ARTICLE

Qian-Zheng-San promotes regeneration after sciatic nerve crush injury in rats

Zhi-Yong Wang[1], Li-Hua Qin[1], Wei-Guang Zhang[1], Pei-Xun Zhang[2,*], Bao-Guo Jiang[2]
1 Department of Anatomy and Histo-embryology, School of Basic Medical Sciences, Peking University, Beijing, China
2 Department of Trauma and Orthopedics, Peking University People's Hospital, Beijing, China

Funding: *This study was supported by the National Natural Science Foundation of China, No. 31571235 (to PXZ), 31771322 (to PXZ), 81401007 (to ZYW); the National Key Basic Research Program of China (973 Program), No. 2014CB542201 (to PXZ); the Beijing Science and Technology New Star Cross Program of China, No. 2018019 (to PXZ); the Natural Science Foundation of Beijing of China, No. 7162098 (to WGZ); the Fostering Young Scholars of Peking University Health Science Center of China, No. BMU2017PY013 (to PXZ).*

Graphical Abstract

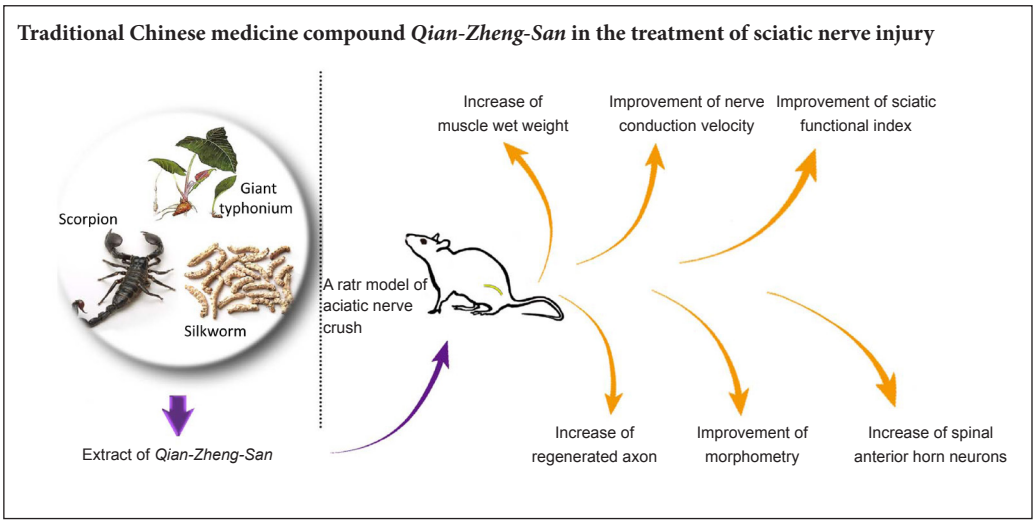

Correspondence to:
Pei-Xun Zhang, MD, PhD, zhangpeixun@126.com.

orcid:
0000-0002-8379-1607 (Pei-Xun Zhang)

doi: *10.4103/1673-5374.247472*

Received: *August 23, 2018*
Accepted: *September 25, 2018*

Abstract

Qian-Zheng-San, a traditional Chinese prescription consisting of *Typhonii Rhizoma*, *Bombyx Batryticatus*, *Scorpio*, has been found to play an active therapeutic role in central nervous system diseases. However, it is unclear whether *Qian-Zheng-San* has therapeutic value for peripheral nerve injury. Therefore, we used Sprague-Dawley rats to investigate this. A sciatic nerve crush injury model was induced by clamping the right sciatic nerve. Subsequently, rats in the treatment group were administered 2 mL *Qian-Zheng-San* (1.75 g/mL) daily as systemic therapy for 1, 2, 4, or 8 weeks. Rats in the control group were not administered *Qian-Zheng-San*. Rats in sham group did not undergo surgery and systemic therapy. Footprint analysis was used to assess nerve motor function. Electrophysiological experiments were used to detect nerve conduction function. Immunofluorescence staining was used to assess axon counts and morphological analysis. Immunohistochemical staining was used to observe myelin regeneration of the sciatic nerve and the number of motoneurons in the anterior horn of the spinal cord. At 2 and 4 weeks postoperatively, the sciatic nerve function index, nerve conduction velocity, the number of distant regenerated axons and the axon diameter of the sciatic nerve increased in the *Qian-Zheng-San* treatment group compared with the control group. At 2 weeks postoperatively, nerve fiber diameter, myelin thickness, and the number of motor neurons in the lumbar spinal cord anterior horn increased in the *Qian-Zheng-San* treatment group compared with the control group. These results indicate that *Qian-Zheng-San* has a positive effect on peripheral nerve regeneration.

Key Words: *nerve regeneration; traditional Chinese medicine; crush injury; peripheral nerve regeneration; nerve conduction velocity; sciatic function index; nerve injury; nerve repair; formula; scorpion; neural regeneration*

Chinese Library Classification No. *R563; R364*

Introduction

Following peripheral nerve injury, the distal nerve segment undergoes Wallerian degeneration, the distal nerve fibers gradually disintegrate, and the debris is eventually cleared by Schwann cells and macrophages. Being stimulated by the damage, local expression of neurotrophic factors increases, but is insufficient to effectively induce the regeneration of proximal axons or for the recovery of neurological structure or function (He et al., 2016). The corresponding neurons degenerate or die because of the interruption of axoplasmic transport (Wang et al., 2018a). Therefore, to give a drug with neuroprotective effect as adjuvant therapy is particularly necessary for regeneration after nerve injury.

Qian-Zheng-San (QZS), a classic formula of traditional

Chinese medicine, consisting of Typhonii Rhizoma, Bombyx Batryticatus, Scorpio, has been shown to exhibit neuroprotective effects in mouse models of Parkinson's disease, preventing the loss of substantia nigra dopamine neurons, protecting mitochondrial function, decreasing mtDNA damage and synergistically upregulating the mRNA expression of NADH dehydrogenase 1 (ND1) (He et al., 2010; Zhang et al., 2013; Gong et al., 2014). In many kinds of peripheral nerve injury models, including nerve crush injury models, neuronal death always follows nerve injuries, hindering nerve regeneration and functional recovery (West et al., 2007, 2013; Catapano et al., 2017). QZS may improve the symptoms of facial paralysis when combined with Ginger moxibustion (Yang, 2010). QZS also has a significant therapeutic effect on prosopalgia. Scorpion, one of the three components of QZS, exerts a direct effect on excitable membranes (Adam et al., 1966), and influences kinetics of the reaction with sodium channels of nodes of Ranvier (Mozhaeva and Naumov, 1980). These findings suggest that QZS, or its components, may have a positive effect on peripheral nerve regeneration after injury. Therefore, in this study QZS was administered to a sciatic nerve crush injury model, one of the commonly used models of nerve injury (Renno et al., 2015; Yang et al., 2015), to preliminarily investigate its effects on peripheral nerve regeneration after crush injury.

In the past, QZS has been applied to central and cranial nerve injury models, but there were no reports of its usefulness for spinal nerve injury. QZS was applied to the spinal nerve crush injury model in this experiment, aiming to broaden its application range and to better understand its potential therapeutic role.

Materials and Methods

Drug preparation and treatment protocol

The composition of QZS was as follows (with voucher numbers): giant typhonium tuber (QZS01-120306) 60 g, stiff silkworm (QZS02-120306) 60 g, and Chinese scorpion (QZS03-120306) 60 g. All medicines were purchased from Tong Ren Tang Drugstore in Beijing, China and authenticated by experts in pharmacognosy. Decoctions were prepared according to the classic 1:1:1 ratio (by weight) and mixed well. The components were decocted with 10 volumes of distilled water for 2 hours, and the supernatant was decanted and saved. Subsequently, the same volume of fresh water was used for the second decoction for 1 hour, and the two supernatants were then combined and mixed, according to the method described previously (Wang et al., 2013a, b). Finally, the QZS preparation was concentrated to 1.75 g total dry weight of the crude component per milliliter of decoction.

According to the standard dosages of the formula in humans, the equivalent dose for rats, based on body weight, was calculated (Wojcikowski, 2014). Starting from the first day following surgery, rats treated with QZS were given 2 mL of QZS solution by oral gavage every day for 1, 2, 4 or 8 weeks, while animals in the NCI and sham groups were given 2 mL of distilled water by oral gavage every day at the same time points.

Animals

Eighteen male specific-pathogen-free Sprague-Dawley rats weighing 210–230 g and aged two months old (animal license number: SYXK (Jing) 2016-0041) were used in this study. The animals were sourced from Beijing Vital River Laboratory Animal Technology Co., Ltd. (Beijing, China) and maintained under specific pathogen-free laboratory conditions under a 12-hour light/dark cycle, with free access to pellet food and water.

The rats were randomly separated into three groups ($n = 6$): sham group (sham surgery), nerve crush injury (NCI) group (nerve crush injury only), and nerve crush injury + QZS group (NCI + QZS group, nerve crush injury followed by QZS treatment). Every effort was made to minimize animal suffering and reduce the number of animals used. All procedures were performed in strict conformity with the National Institution of Health Guide for the Care and Use of Laboratory Animals (NIH Publication number 85-23, revised 1985) and the related ethics regulations of Peking University. The study was approved by Animal Ethics Committee of Peking University (approval number: LA2017128) on June 1, 2017.

Surgical procedures

Rats in the nerve crush injury model were anesthetized using sodium pentobarbital water solution (30 mg/kg, intraperitoneally). After anesthesia the skin in the right thigh area was sterilized and the right sciatic nerve exposed. At the site 10 mm proximal to the main bifurcation for the tibial and peroneal nerves, a toothless vessel clamp was used to crush the sciatic nerve for 60 seconds (the degree of crush was two teeth bitten in the handles), and then the clamping site was marked with a 10-0 microscopic suture under aseptic conditions (Răducan et al., 2013; Kou et al., 2013; Demir et al., 2014; Wang et al., 2014, 2018b). To monitor the crush injury, electrophysiological assessments (MedlecSynergy, 04oc003, Oxford Instrument Inc., Oxford, UK) were conducted. Two pairs of electrodes were used to record compound action potentials, and upon progressive decrease to 0 mV, induction of the model was considered successful. The wound was closed and disinfected with 70% alcohol. Rats in the sham group did not experience crush injury, after being anesthetized, the nerves were exposed and the incision was sutured. All rats were put back into their cages and raised with normal food and water. Tissues were harvested and examined at postoperative 1, 2, 4, or 8 weeks.

Walking track analysis

At 1, 2, 4, and 8 weeks after the procedure, footprint analysis was performed as described previously (Zhang et al., 2014). A custom-made walking box (12 cm × 50 cm), with one end closed, was used. White paper (12 cm × 50 cm) lined the bottom of the track. The bilateral hind feet were coated with black pigment, then the rat was put at the door of the walking box. Each rat was then allowed to walk in the box three

or four times, and the bilateral footprints were recorded. Clear and complete prints were chosen for further analysis. Print length (PL), toe spread (TS), and intermediary toe spread (IT) were measured. The left foot parameters were recorded as normal PL (NPL), normal TS (NTS), and normal IT (NIT); the right foot parameters were recorded as experimental PL (EPL), experimental TS (ETS), and experimental IT (EIT). A sciatic function index (SFI) was calculated using the following formula: SFI = −38.3 ([EPL − NPL]/NPL) + 109.5 ([ETS − NTS]/NTS) + 13.3 ([EIT−NIT]/NIT) − 8.8.

Electrophysiological examination

An electrophysiological instrument (MedlecSynergy, 04oc003, Oxford Instrument Inc.) was used to assess sciatic nerve electrophysiology eight weeks following surgery. The stimulating electrode was successively placed on both sides of the injury site. The recording electrode was inserted into the triceps surae muscle and the ground electrode inserted into the subcutaneous tissue between the two electrodes. Rectangular pulses (duration 0.1 ms, 0.9 mA, 10 Hz, six continual stimuli) were used. Nerve conduction velocity (NCV) was calculated semi-automatically by dividing the distance between the two stimulating sites by the difference in the conduction time.

Wet weight of the triceps surae muscle and muscle histological analysis

The total mass of the triceps surae muscle was measured after electrophysiological examination. Triceps surae muscles were freed and harvested from both sides of the hind legs. Nerves, blood vessels, and the deep fascia covering the surface of the muscle were stripped off and discarded. To reduce statistical error and ensure objectivity, the triceps surae muscles used for analysis included the tendons. Muscles were then immediately weighed with a microbalance. The recovery rate of muscle wet weight was obtained by the following equation: Recovery rate = wet weight of the operated muscle/wet weight of the unoperated muscle.

After being weighed, each triceps surae muscle was then put in 4% paraformaldehyde for one week, then individually rinsed in water, dehydrated through a graded series of ethanol washes, immersed in xylene, and embedded in paraffin. Each muscle segment was sliced into 5-μm-thick cross sections, and then stained in hematoxylin-eosin solution. Images were acquired under a dissecting microscope (Leica, MZ75, Bensheim, Germany), from which the cross sectional area of muscle cells was measured using Image-Pro Plus 6.0 software (Media Cybernetics Inc., Rockville, MD, USA).

Neurohistological analysis

Sciatic nerves were harvested from each rat and the nerve segment cut 3 mm distal to the crush site. Each segment was then divided into two sections for histological analysis separately as follows.

Axonal staining by immunofluorescence: Each tissue was put in 4% paraformaldehyde for 6 hours, incubated in 30% sucrose overnight at 4°C, embedded at the optimal cutting temperature, frozen at −80°C, and sliced into 15-μm-thick cross sections using a frozen slicer (Leica, CM1950). Frozen sections were washed in phosphate buffered saline (PBS), blocked in goat serum, washed in PBS, incubated with anti-NF-200 antibodies (1:300; Sigma, St. Louis, MO, USA) at 37°C for 2 hours, and then incubated with tetramethylrhodamine-conjugated secondary antibodies (1:800; Sigma) for 1.5 hours at 37°C. Each section was visualized using a microscope, from which regenerated axons were counted using ImageJ software v1.47 (NIH, Bethesda, MD, USA).

Myelin staining by osmium tetroxide: Tissues were fixed in paraformaldehyde for 12 hours and immersed in water for 9 hours. The segments were stained in 1% osmium tetroxide for 12 hours, dehydrated through a graded ethanol series, immersed in xylene and embedded using paraffin, and then sliced into 5-μm-thick cross sections using a cryostat (Leica). Images were acquired at 400× magnification using a dissecting microscope. The axon and fiber diameters were measured using ImageJ software. Myelin thickness and g-ratio were calculated as follows: myelin thickness = (fiber diameter − axon diameter)/2; g-ratio = axon diameter/fiber diameter.

Neuronal staining of spinal ventral horn

Neuronal viability was evaluated using immunohistochemistry and the monoclonal antibody NeuN (Abcam, Birmingham, UK). Paraffin transversal sections were deparaffinized and dehydrated. Antigen retrieval was performed, and endogenous peroxidase was blocked using hydrogen peroxide. Histological sections were incubated for 2 hours in a humid dark chamber with the primary antibody anti-NeuN (1:200). The secondary antibody (1:500; rabbit-derived polyclonal antibody; Abcam) was added, and the sections were incubated for 30 minutes. The reactions were developed with 3-3′ diaminobenzidine peroxidase (ZSGB, Beijing, China). The sections were washed in water, dehydrated, and mounted on slides with coverslips. Counting of the neuronal bodies was performed using Image-Pro Plus 6.0 software.

Statistical analysis

Statistical analyses were performed using SPSS 13.0 software (SPSS, Chicago, IL, USA). All data are expressed as the mean ± standard deviation (SD). One-way analysis of variance was utilized to compare the number of axons and spinal cord neurons, axon diameter, fiber diameter, g-ratio, SFI, myelin thickness, and NCV in all groups, and the least significant difference test was used as a *post hoc* test for intergroup comparisons. Independent sample *t*-tests were also used to compare the recovery rate of muscle wet weight between the NCI and NCI + QZS groups. $P < 0.05$ was considered significant.

Results

QZS effect on the recovery of hindlimb motor function

As shown in **Figure 1**, SFIs in the NCI and NCI + QZS groups were significantly lower than in the sham group 1

week after surgery ($P < 0.05$). SFIs did not significantly differ between the NCI and NCI + QZS groups at this time. At 2 and 4 weeks after surgery, SFIs in the NCI and NCI + QZS groups were significantly lower than in the sham group ($P < 0.05$), and higher in the NCI + QZS group than in the NCI group ($P < 0.05$). At 8 weeks following surgery, the NCI group had significantly lower SFI than the sham group ($P < 0.05$). The values were not different between the NCI and NCI + QZS groups.

QZS effects on electrophysiological parameters of injured sciatic nerves

As shown in **Figure 2**, 2 and 4 weeks after surgery, NCVs were obviously lower in the NCI and NCI + QZS groups than in the sham group ($P < 0.05$), and higher in rats treated with QZS than in rats without the drug ($P < 0.05$). At 8 weeks after surgery, NCVs were significantly lower in the NCI and NCI + QZS groups than in the sham group ($P < 0.05$), while there was no obvious difference between the two nerve crush injury groups.

QZS effect on triceps surae muscle wet mass recovery

As shown in **Figure 3**, 1, 2, and 4 weeks postoperatively, the recovery rates of muscle wet weight did not differ between the NCI and NCI + QZS groups. At 8 weeks after surgery, the recovery rate of muscle wet weight in the NCI + QZS group was heavier than in the NCI group ($P < 0.05$). In general, the recovery rate in the NCI + QZS groups was greater than in the NCI group.

As shown in **Figure 4**, the muscle fibers in the sham group remained steady over time, with polygonal morphology, while the muscle fibers in the NCI and NCI + QZS groups were irregular oval or round. The muscle fiber area in the NCI and NCI + QZS groups looked less than in the sham group during the same period. The muscle fiber area in the NCI + QZS group looked greater than in the NCI group. In general, the muscle fiber area in the NCI and NCI + QZS groups tended to gradually increase over time.

Effect of QZS on regeneration of sciatic nerve fibers

As shown in **Figure 5A**, the axons in the sham group evenly distributed at each time point, while the axons in the NCI and NCI + QZS groups were not. The density of axons in the NCI and NCI + QZS groups appeared less than in the sham group during the same period. In general, the density of axons in each group gradually increased over time.

As shown in **Figure 5B**, 2 and 4 weeks postoperatively, the number of regenerated axons in the sham group was higher than in the NCI and NCI + QZS groups ($P < 0.05$), while the number of regenerated axons in the NCI + QZS groups was higher than in the NCI group ($P < 0.05$). At 8 weeks after surgery, the numbers of regenerated axons in the NCI and NCI + QZS groups were higher than in the sham group ($P < 0.05$), while there was no difference between the NCI and NCI + QZS groups.

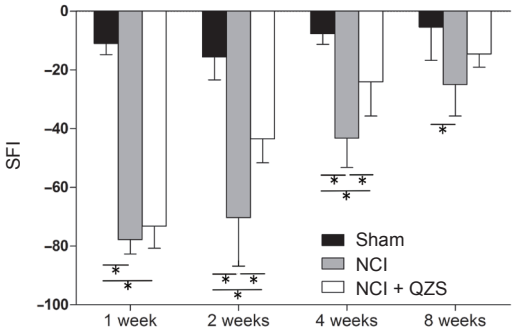

Figure 1 Effect of QZS on the recovery of hindlimb motor function in sciatic nerve injury rats.
A higher SFI means the better funtion of the sciatic nerve. SFIs in the NCI and NCI + QZS groups were significantly lower than that in the sham group 1 week after surgery. Two and 4 weeks after surgery, SFIs in the NCI and NCI + QZS groups were significantly lower than in the sham group, and higher in the NCI + QZS group than in the NCI group. Eight weeks later, the SFI in the NCI group was significantly lower than that in the sham group. $*P < 0.05$. Data are expressed as the mean ± SD ($n = 6$; one-way analysis of variance followed by the least significant difference *post hoc* test). QZS: *Qian-Zheng-San*; SFI: sciatic function index; NCI: nerve cush injury.

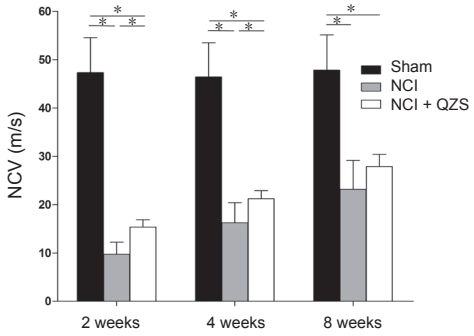

Figure 2 Effect of QZS on electrophysiological parameters of injured sciatic nerves in rats.
Two and four weeks after surgery, NCVs were significantly lower in the NCI and NCI + QZS groups than in the sham group, and higher in rats treated with QZS than in those without the drug. At 8 weeks after surgery, NCVs were significantly lower in the NCI and NCI + QZS groups than in the sham group. $*P < 0.05$. Data are expressed as the mean ± SD ($n = 6$; one-way analysis of variance followed by the least significant difference *post hoc* test). QZS: *Qian-Zheng-San*; NCV: nerve conduction velocity; NCI: nerve cush injury.

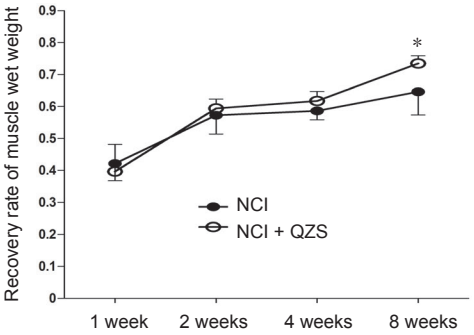

Figure 3 Effect of QZS on wet mass recovery of triceps surae muscle in sciatic nerve injury rats.
At 8 weeks after surgery, the recovery mass in the NCI + QZS group was higher than that in the NCI group. In general, the recovery rate in the NCI + QZS group was greater than that in the NCI group. $*P < 0.05$, *vs.* NCI group. Data are expressed as the mean ± SD ($n = 6$; independent sample *t*-test). QZS: *Qian-Zheng-San*; NCI: nerve cush injury.

QZS effect on myelin morphology of sciatic nerve injury

As shown in **Figure 6**, 4 weeks postoperatively, in the sham group there was substantial and evenly distributed myelin, with the myelin sheaths appearing regular and uniform. In the NCI group, myelin regeneration appeared poor, and the distribution was uneven. The myelin sheaths appeared to have a relatively small diameter and thickness. In the NCI + QZS groups, myelin regeneration was poor, but the myelin density seemed higher compared to the NCI group. The myelin sheaths had a small diameter and thickness. At 8 weeks after surgery, myelin regeneration in the sham group was similar to that in the same group 4 weeks after surgery. In the NCI and NCI + QZS groups, myelin sheaths appeared to have a mature structure. The distribution of the myelin sheaths looked uniform, with normal structure. The diameters of the myelin sheaths generally appeared small.

Morphometric measurements were performed for each group. As shown in **Figure 7A**, 2 and 4 weeks after surgery, axon diameter was significantly larger in the sham group than in the NCI and NCI + QZS groups ($P < 0.05$), and significantly larger in rats treated with QZS than in those without treatment ($P < 0.05$). At 8 weeks after surgery, axon diameter was significantly larger in the sham group than in the NCI and NCI + QZS groups ($P < 0.05$). As shown in **Figure 7B**, 2 weeks after surgery, the fiber diameter was significantly greater in the sham group than in the NCI and NCI + QZS groups ($P < 0.05$), and greater in the NCI + QZS group than in the NCI group ($P < 0.05$). At 4 and 8 weeks after surgery, fiber diameter in the sham group was significantly greater than in the NCI and NCI + QZS groups ($P < 0.01$). As shown in **Figure 7C**, 2 and 4 weeks after surgery, g-ratios did not differ statistically between any pairwise comparison between the three groups. At 8 weeks after surgery, g-ratio was significantly higher in the NCI + QZS group than in the sham group ($P < 0.05$). As shown in **Figure 7D**, 2 weeks after surgery, myelin thickness was significantly greater in the sham group than in the NCI and NCI + QZS groups ($P < 0.05$), and greater in the NCI + QZS group than in the NCI group ($P < 0.05$). At 4 and 8 weeks after surgery, myelin thickness in the sham group was significantly greater than that in the NCI and NCI + QZS groups ($P < 0.01$).

QZS effect on the number of motoneurons in the anterior horn of the lumbar spinal cord

At 2 weeks after surgery, the number of neurons was greater in the sham group than in the NCI and NCI + QZS groups ($P < 0.05$), and greater in the NCI + QZS group than in the NCI group ($P < 0.05$). At 4 weeks after surgery, the number of neurons was greater in the sham group than in the NCI and NCI + QZS groups ($P < 0.05$); however, there was no difference between the NCI and NCI + QZS groups (**Figure 8**).

Discussion

This study using nerve crush injury models suggests that QZS has a positive effect on recovery from this injury. SFI, NCV, the number of regenerated axons, and axon diameter were higher in the NCI + QZS group than in the NCI group 2 and 4 weeks postoperatively. Fiber diameter, myelin thickness, and the number of neurons in the spinal anterior horn in the NCI + QZS group were significantly better than in the NCI group 2 weeks after surgery. These findings suggest that QZS promotes structural and functional recovery of the sciatic nerve at early stages after nerve crush injury. At 8 weeks postoperatively, the recovery of muscle wet weight was higher in the NCI + QZS group than that in the NCI group, suggesting that QZS plays a positive role in effecting recovery during late stages of nerve crush injury. Interestingly, the number of regenerated axons was greater in the NCI and NCI + QZS groups than in the sham group 8 weeks postoperatively. It is speculated that the nerve amplification effect, *i.e.*, that one axon of a proximal nerve can emit a number of newborns during regeneration, growing towards the distal end, so there are more fibers in the NCI and NCI + QZS groups than in the sham group, may be at play (Jiang et al., 2006, 2007; Zhang et al., 2009, 2011; Wang et al., 2013a,b, 2013). However, nerve function in the NCI and NCI + QZS groups was inferior to those in the sham group, indicating that not all of these new fibers are able to work; redundant nerve fibers will likely degrade and the number of fibers will reduce to a normal (or lower) level.

The mechanisms underlying the therapeutic actions of QZS are likely complex. QZS regulates the mitoKATP channel to achieve the function of neuron protection through antagonizing the upregulation of SUR1 (Gong et al., 2014). Immune factors and immune cells show a positive effect on nerve regeneration. Typhonii Rhizoma, one ingredient of QZS, stimulates mouse spleen cells and human lymphocytes, and then regulates immunological function (Shan et al., 2001). This may be one of the mechanisms by which QZS promotes nerve regeneration. After peripheral nerve injury, myelin undergoes degeneration and necrosis, and the relevant debris needs to be cleared in time to facilitate fiber regeneration. The lymphocytes activated by Typhonii Rhizoma will remove the debris, acting synergistically with macrophages and thereby accelerating nerve regeneration. Scorpio, another component of QZS, contains a type of polypeptide toxin, scorpion venom component III, which protects dopaminergic neurons of the SN pars compacta region of midbrain. In this study, QZS may also protect the associated neurons of the lumbar spinal cord given the finding that the number of neurons in the NCI + QZS group was higher than in the NCI group 2 weeks after surgery. The mechanisms by which QZS promotes nerve regeneration may be multifaceted. In future research, the chemical constituents of QZS should be isolated and investigated individually.

In this study, QZS had a positive effect on peripheral nerve regeneration, improved structural and functional recovery to a certain extent, and protected the associated neurons from death. This suggests that its application can be extended to peripheral nerve injury.

In the past several years, many studies have focused on the administration of neurotrophic factors to the injured nerve (Hu et al., 2009; Gordon, 2010; Wood et al., 2010; Allen et al., 2013; Huang et al., 2013; Shakhbazau et al., 2013; Sacchetti and Lambiase, 2017; Zhang et al., 2017). For example, nerve growth factor has positive effects on neural survival, development and function (Huang and Reichardt, 2001; Sun

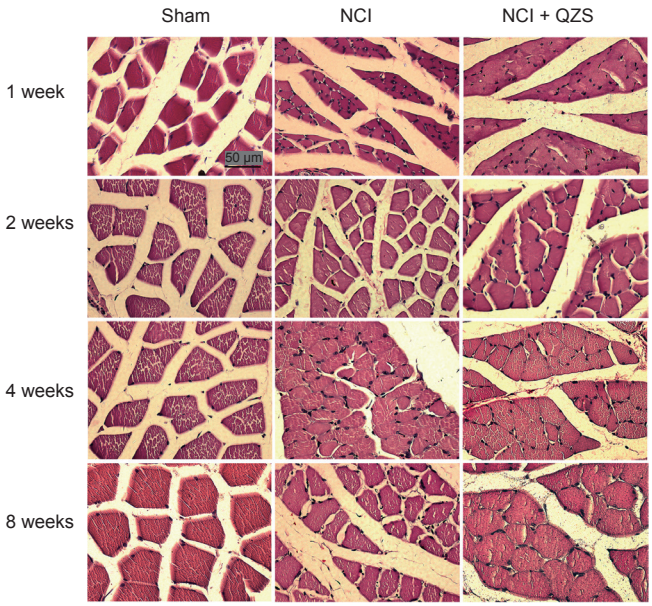

Figure 4 Effect of QZS on the morphology of triceps surae muscle in sciatic nerve injury rats (hematoxylin-eosin staining).
At each time point, the muscle fibers in the sham group are similar, with polygonal morphology, while the muscle fibers in the NCI and NCI + QZS groups are irregular ovals or round. The areas of muscle fibers in the NCI and NCI + QZS groups appear less than in the sham group at the same timepoint. The area of the muscle fibers in the NCI + QZS group appears to be greater than in the NCI group. In general, the muscle fibers area in the NCI and NCI + QZS groups gradually increased with time. Original magnification, 400×; scale bar: 50 μm. QZS: *Qian-Zheng-Sa*n.

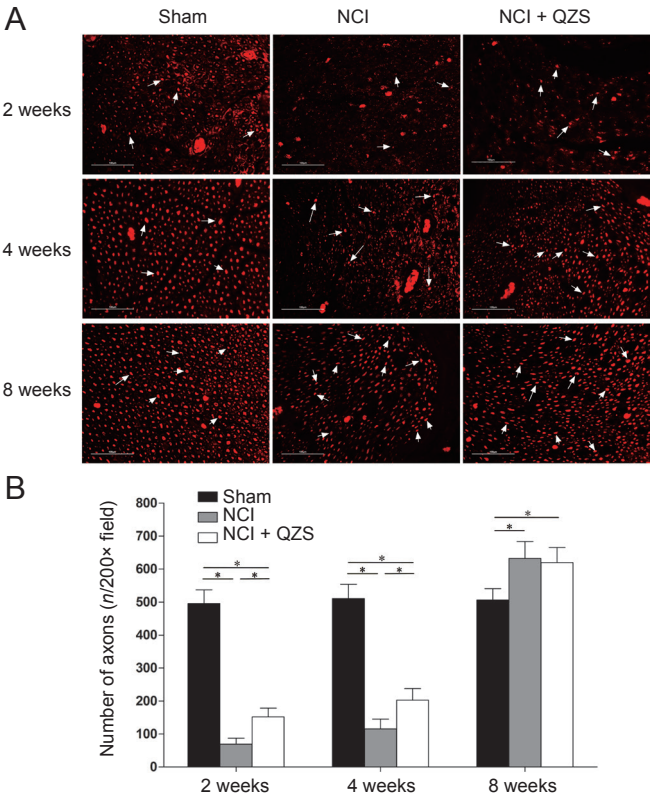

Figure 5 Effect of QZS on regeneration of sciatic nerve fibers in injured rats.
(A) Morphology of nerve axons: Immunofluorescence staining of neurofilament-200; original magnification, 200×; scale bars: 100 μm; red tissue indicates fluorescence coloration of tetramethylrhodamine-conjugated secondary antibodies. Black area indicates background. White arrow indicates positive cells. (B) Count of regenerated nerve axons: 2 and 4 weeks postoperatively, the number of regenerated axons in the sham group was greater than in the NCI and NCI + QZS groups, while the number of regenerated axons in the NCI + QZS group was greater than in the NCI group. At 8 weeks after surgery, the numbers of regenerated axons in the NCI and NCI + QZS groups were greater than those in the sham group. $*P < 0.05$. Data are expressed as the mean ± SD ($n = 6$; one-way analysis of variance followed by the least significant difference *post hoc* test). QZS: *Qian-Zheng-San*.

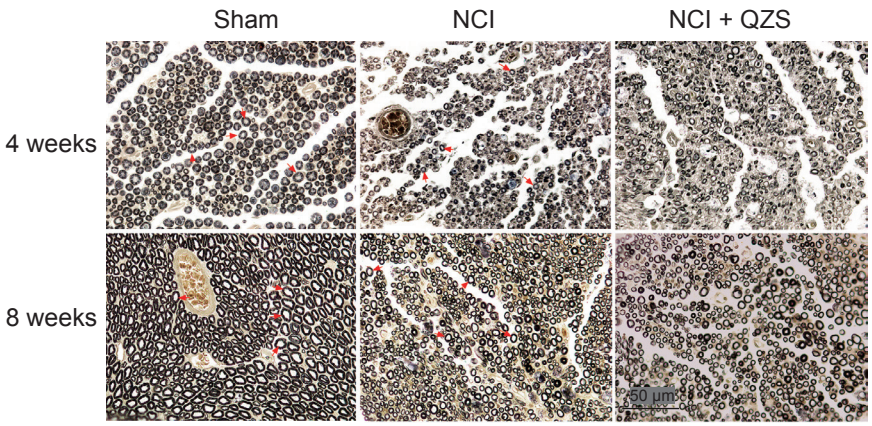

Figure 6 Effect of QZS on myelin morphology of sciatic nerve in injured rats (osmium tetroxide staining).
At 4 weeks postoperatively, in the sham group there is substantial and evenly distributed myelin, and the myelin sheaths appear regular and uniform. In the NCI group, myelin regeneration appears poor, and the myelin sheaths have relatively small diameters and thickness. In the NCI + QZS group, myelin regeneration appears poor, but myelin density is greater compared to the NCI group. At 8 weeks after surgery, myelin regeneration in the sham group showed good regeneration. In the NCI and NCI + QZS groups, the myelin sheaths appear to have a mature structure. The distribution of the myelin sheaths looks uniform, with normal structures. The diameters of myelin sheaths generally appear small. Original magnification, 400×; Scale bar: 50 μm; red arrow indicates myelin. QZS: *Qian-Zheng-San*.

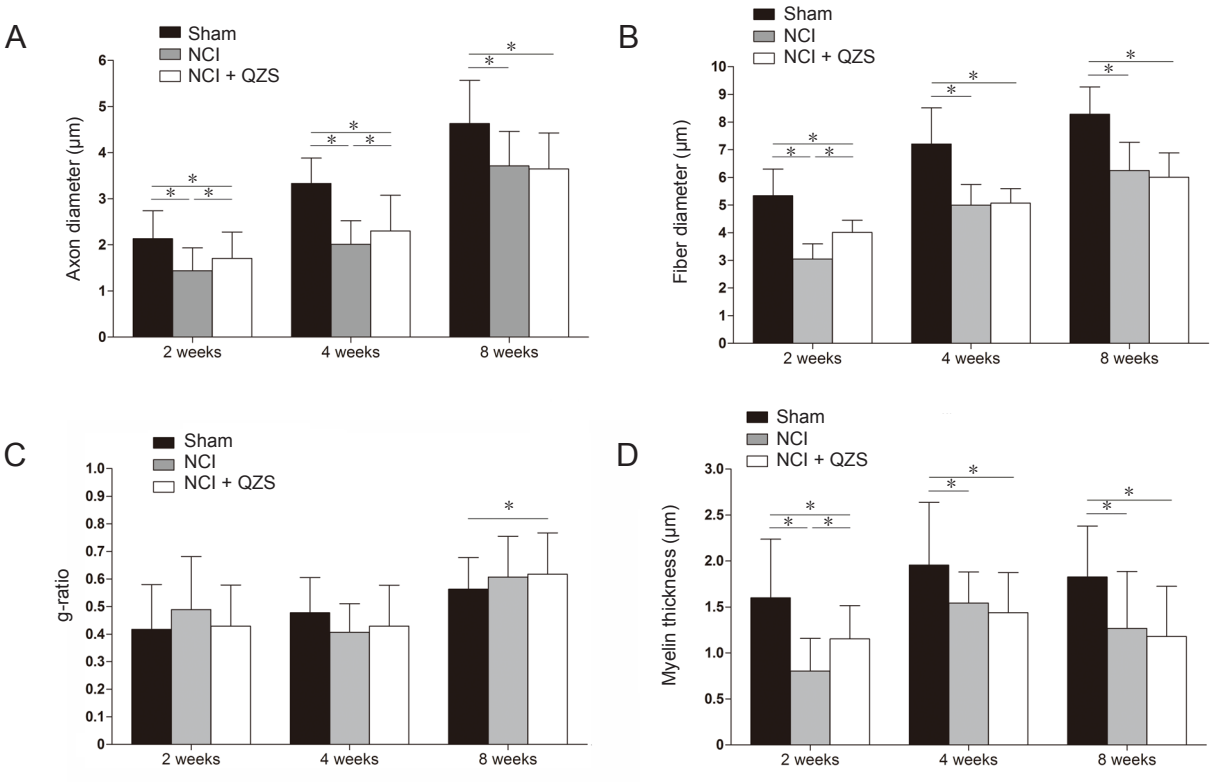

Figure 7 Effect of QZS on morphological parameters of sciatic nerves in injured rats.
(A) Axon diameter: 2 and 4 weeks after surgery, axon diameters were significantly greater in the sham group than in the NCI and NCI + QZS groups, and greater in rats treated with QZS than in rats without treatment. At 8 weeks after surgery, the axon diameter was significantly greater in the sham group than in the NCI and NCI + QZS groups. (B) Fiber diameter: 2 weeks after surgery, fiber diameter was significantly greater in the sham group than in the NCI and NCI + QZS groups, and larger in the NCI + QZS group than in the NCI group. At 4 and 8 weeks after surgery, the fiber diameter in the sham group was significantly greater than in the NCI and NCI + QZS groups. (C) g-ratio: 8 weeks after surgery, the g-ratio in the NCI + QZS group was significantly greater than in the sham group. (D) Myelin thickness: Two weeks after surgery, myelin thickness was significantly greater in the sham group than that in the NCI and NCI + QZS groups, and greater in the NCI + QZS group than in the NCI group. At 4 and 8 weeks after surgery, the myelin thickness in the sham group was significantly greater than in the NCI and NCI + QZS groups. $*P < 0.05$. Data are expressed as the mean ± SD ($n = 6$; one-way analysis of variance followed by the least significant difference *post hoc* test). QZS: *Qian-Zheng-San*.

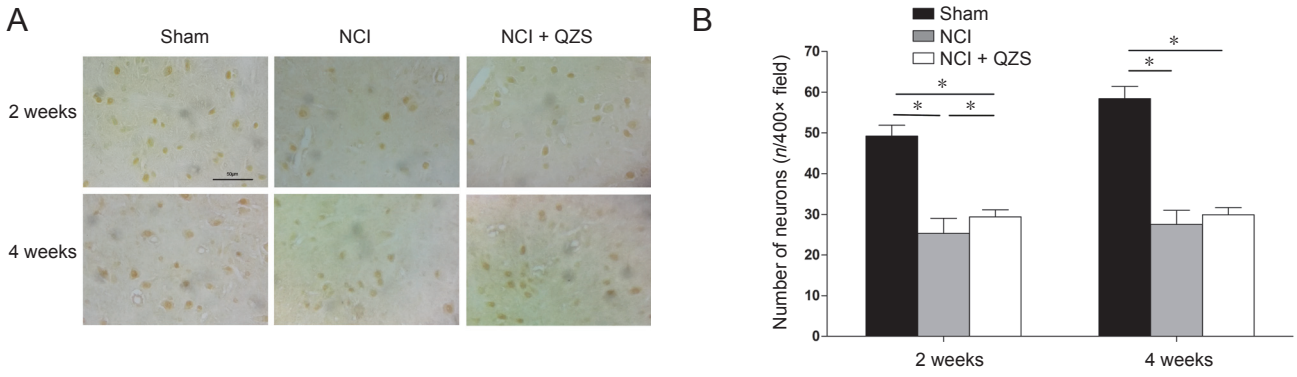

Figure 8 Effect of QZS on the number of motoneurons in the anterior horn of lumbar spinal cord in sciatic nerve injury rats.
(A) Histomorphology of neurons in spinal anterior horn. Immunohistochemical staining; Original magnification, 400×; Scale bar: 50 μm. (B) Count of spinal anterior horn neurons. At 2 weeks after surgery, the number of neurons was greater in the sham group than in the NCI and NCI + QZS groups, and greater in the NCI + QZS group than in the NCI group. At 4 weeks after surgery, the number of neurons was greater in the sham group than in the NCI and NCI + QZS groups. $*P < 0.05$. Data are expressed as the mean ± SD ($n = 6$; one-way analysis of variance followed by the least significant difference *post hoc* test). QZS: *Qian-Zheng-San*.

et al., 2009; Chen et al., 2010). However, nerve growth factor also has some inevitable shortcomings and degrades rapidly in solution, because its half-life period is short it is difficult to maintain at local sites (Tria et al., 1994; Tsai et al., 2003), and systemic application can cause hyperalgesia (Lewin et al., 1994). Thus, traditional Chinese medicine, such as QZS, may be used as a substitute because it contains multiple active ingredients which might avoid or weaken the disadvantages mentioned above.

It is noteworthy that the nerve function in the NCI + QZS group was inferior to that in the sham group. The reason may be that the concentration of the drug solution is small, or that systemic treatment by oral gavage makes it impossible for the drug to concentrate at the injury site. To further improve nerve regeneration, concentration of the drug solution, microspheres used for controlled targeting and release (Yu et al., 2009; Wood et al., 2013; Zeng et al., 2014; Roam et al., 2015; Li et al., 2016; Ni et al., 2016; Zhuang et al., 2016; Si et al., 2017), and local injection will be investigated in future experiments.

QZS, as a traditional Chinese medicine formulation, inevitably has some limitations. Traditional Chinese medicines, such as QZS, contain many ingredients, and the active ingredients that promote nerve regeneration are unclear. These need to be identified, isolated and recombined in future studies to explore the synergistic effects of effective compounds.

In this study, the nerve crush model was used. Crush injury is partial damage, in which the nerve recovery cycle is shorter. In this model, endoneurial tubes remain intact, ensuring that proximal axons grow distally along these conduits. Consequently, nerve regeneration following crush injury is superior to that after injury in which endoneurial tubes are transected. At 8 weeks postoperatively, regeneration of sciatic nerves had been almost completed in the NCI and NCI + QZS groups, and most of the test results in the NCI and NCI + QZS groups were not statistically different.

The results of this study indicate potential clinical application prospects in nerve injury induced by traffic trauma, mechanical trauma and other external damage, which needs further experimental research to verify.

Acknowledgments: *We thank Long Tian and Jing Fan from Health Science Center, Peking University, China for providing experimental facilities.*

Author contributions: *Study design and supervision: PXZ and BGJ; experiment implementation: ZYW; data analysis: LHQ and WGZ; paper writing: ZYW. All authors approved the final version of the paper.*

Conflicts of interest: *None declared.*

Financial support: *This study was supported by the National Natural Science Foundation of China, No. 31571235 (to PXZ), 31771322 (to PXZ), 81401007 (to ZYW); the National Key Basic Research Program of China (973 Program), No. 2014CB542201 (to PXZ); the Beijing Science and Technology New Star Cross Program of China, No. 2018019 (to PXZ); the Natural Science Foundation of Beijing of China, No. 7162098 (to WGZ); the Fostering Young Scholars of Peking University Health Science Center of China, No. BMU2017PY013 (to PXZ). The funding bodies played no role in the study design, in the collection, analysis and interpretation of data, in the writing of the paper, and in the decision to submit the paper for publication.*

Institutional review board statement: *The study was approved by the Animal Ethics Committee of Peking University of China (approval number: LA2017128) on June 1, 2017. All experimental procedures described here were in accordance with the National Institutes of Health (NIH) guidelines for the Care and Use of Laboratory Animals.*

Copyright license agreement: *The Copyright License Agreement has been signed by all authors before publication.*

Data sharing statement: *Datasets analyzed during the current study are available from the corresponding author on reasonable request.*

Plagiarism check: *Checked twice by iThenticate.*

Peer review: *Externally peer reviewed.*

Open peer reviewer: *Melanie G. Urbanchek, University of Michigan, USA.*

Additional file: *Open peer review report 1.*

References

Adam KR, Schmidt H, Stampfli R, Weiss C (1966) The effect of scorpion venom on single myelinated nerve fibres of the frog. Br J Pharmacol Chemother 26:666-677.

Allen SJ, Watson JJ, Shoemark DK, Barua NU, Patel NK (2013) GDNF, NGF and BDNF as therapeutic options for neurodegeneration. Pharmacol Ther 138:155-175.

Catapano J, Zhang J, Scholl D, Chiang C, Gordon T, Borschel GH (2017) N-acetylcysteine prevents retrograde motor neuron death after neonatal peripheral nerve injury. Plast Reconstr Surg 139:1105-1115.

Chen J, Chu YF, Chen JM, Li BC (2010) Synergistic effects of NGF, CNTF and GDNF on functional recovery following sciatic nerve injury in rats. Adv Med Sci 55:32-42.

Demir R, Yayla M, Akpinar E, Cakir M, Calikoglu C, Ozel L, Ozdemir G, Mercantepe T (2014) Protective effects of alpha-lipoic acid on experimental sciatic nerve crush injury in rats: assessed with functional, molecular and electromicroscopic analyses. Int J Neurosci 124:935-943.

Gong XG, Sun HM, Zhang Y, Zhang SJ, Gao YS, Feng J, Hu JH, Gai C, Guo ZY, Xu H, Ma L (2014) Da-Bu-Yin-Wan and Qian-Zheng-San to neuroprotect the mouse model of Parkinson's disease. Evid Based Complement Alternat Med 2014:729195.

Gordon T (2010) The physiology of neural injury and regeneration: The role of neurotrophic factors. J Commun Disord 43:265-273.

He X, Gao YS, Sun HM, Wu HX, Xu H, Wang ZY (2010) Effect of Dabuyin Pill and Qianzheng Powder on activity of mitochondrial enzyme complexes in mice with Parkinson's disease. Jiangsu Zhongyi 42:72-73.

He XZ, Wang W, Hu TM, Ma JJ, Yu CY, Gao YF, Cheng XL, Wang P (2016) Peripheral nerve repair: theory and technology application. Zhongguo Zuzhi Gongcheng Yanjiu 20:1044-1050.

Hu X, Huang J, Ye Z, Xia L, Li M, Lv B, Shen X, Luo Z (2009) A novel scaffold with longitudinally oriented microchannels promotes peripheral nerve regeneration. Tissue Eng 15:3297-3308.

Huang EJ, Reichardt LF (2001) Neurotrophins: roles in neuronal development and function. Annu Rev Neurosci 24:677-736.

Huang J, Zhang Y, Lu L, Hu X, Luo Z (2013) Electrical stimulation accelerates nerve regeneration and functional recovery in delayed peripheral nerve injury in rats. Eur J Neurosci 38:3691-3701.

Jiang B, Zhang P, Zhang D, Fu Z, Yin X, Zhang H (2006) Study on small gap sleeve bridging peripheral nerve injury. Artif Cells Blood Substit Immobil Biotechnol 34:55-74.

Jiang BG, Yin XF, Zhang DY, Fu ZG, Zhang HB (2007) Maximum number of collaterals developed by one axon during peripheral nerve regeneration and the influence of that number on reinnervation effects. Eur Neurol 58:12-20.

Kou Y, Wang Z, Wu Z, Zhang P, Zhang Y, Yin X, Wong X, Qiu G, Jiang B (2013) Epimedium extract promotes peripheral nerve regeneration in rats. Evid Based Complement Alternat Med 954798.

Lewin GR, Rueff A, Mendell LM (1994) Peripheral and central mechanisms of NGF-induced hyperalgesia. Eur J Neurosci 6:1903-1912.
Li Q, Li T, Cao XC, Luo DQ, Lian KJ (2016) Methylprednisolone microsphere sustained-release membrane inhibits scar formation at the site of peripheral nerve lesion. Neural Regen Res 11:835-841.
Mozhaeva GN, Naumov AP (1980) Kinetics of the reaction between scorpion toxin and the sodium channels of nodes of Ranvier. Neirofiziologiia 12:619-626.
Ni Q, Chen W, Tong L, Cao J, Ji C (2016) Preparation of novel biodegradable ropivacaine microspheres and evaluation of their efficacy in sciatic nerve block in mice. Drug Des Devel Ther 10:2499-2506.
Răducan A, Mirică S, Duicu O, Răducan S, Muntean D, Fira-Mlădinescu O, Lighezan R (2013) Morphological and functional aspects of sciatic nerve regeneration after crush injury. Rom J Morphol Embryol 54:735-739.
Renno WM, AL-maghrebi M, Rao MS, Khraishah H (2015) (-)-Epigallocatechin-3-gallate modulates spinal cord neuronal degeneration by enhancing growth-associated protein 43, B-cell lymphoma 2, and decreasing B-cell lymphoma 2-associated x protein expression after sciatic nerve crush injury. J Neurotrauma 32:170-184.
Roam JL, Yan Y, Nguyen PK, Kinstlinger IS, Leuchter MK, Hunter DA, Wood MD, Elbert DL (2015) A modular, plasmin-sensitive, clickable poly(ethylene glycol)-heparin-laminin microsphere system for establishing growth factor gradients in nerve guidance conduits. Biomaterials 72:112-124.
Sacchetti M, Lambiase A (2017) Neurotrophic factors and corneal nerve regeneration. Neural Regen Res 12:1220-1224.
Shakhbazau A, Mohanty C, Shcharbin D, Bryszewska M, Caminade AM, Majoral JP, Alant J, Midha R (2013) Doxycycline-regulated GDNF expression promotes axonal regeneration and functional recovery in transected peripheral nerve. J Control Release 172:841-851.
Shan BE, Zhang JY, Li QX (2001) Human T cell and monocyte modulating activity of Rhizoma typhonii in vitro. Zhongguo Zhong Xi Yi Jie He Za Zhi 21:768-772.
Si HB, Zeng Y, Lu YR, Cheng JQ, Shen B (2017) Control-released basic fibroblast growth factor-loaded poly-lactic-co-glycolic acid microspheres promote sciatic nerve regeneration in rats. Exp Ther Med 13:429-436.
Sun W, Sun C, Lin H, Zhao H, Wang J, Ma H, Chen B, Xiao Z, Dai J (2009) The effect of collagen-binding NGF-beta on the promotion of sciatic nerve regeneration in a rat sciatic nerve crush injury model. Biomaterials 30:4649-4656.
Tria MA, Fusco M, Vantini G, Mariot R (1994) Pharmacokinetics of nerve growth factor (NGF) following different routes of administration to adult rats. Exp Neurol 127:178-183.
Tsai CC, Lu MC, Chen YS, Wu CH, Lin CC (2003) Locally administered nerve growth factor suppresses ginsenoside Rb1-enhanced peripheral nerve regeneration. Am J Chin Med 31:665-673.
Wang CZ, Chen YJ, Wang YH, Yeh ML, Huang MH, Ho ML, Liang JI, Chen CH (2014) Low-level laser irradiation improves functional recovery and nerve regeneration in sciatic nerve crush rat injury model. PLoS One 9:e103348.
Wang D, Li ZM, Zhao MJ, Xue RH, Xu H, Zhong LM (2018a) Neuroelectrophysiological characteristics of peripheral neuropathy in primary Sjögren's syndrome: study protocol for a prospective case series and pre-preliminary results. Asia Pac J Clin Trials Nerv Syst Dis 2018;3:68-73
Wang Z, Zhang P, Kou Y, Yin X, Han N, Jiang B (2013a) Hedysari extract improves regeneration after peripheral nerve injury by enhancing the amplification effect. PLos One 8:e67921.
Wang Z, Yang X, Zhang W, Zhang P, Jiang B (2018b) Tanshinone IIA attenuates nerve structural and functional damage induced by nerve crush injury in rats. PLoS One 13:e0202532.
Wang ZY, Zhang PX, Han N, Kou YH, Yin XF, Jiang BG (2013b) Effect of modified formula radix hedysari on the amplification effect during peripheral nerve regeneration. Evid Based Complement Alternat Med 2013:647982.
West CA, Davies KA, Hart AM, Wiberg M, Williams SR, Terenghi G (2007) Volumetric magnetic resonance imaging of dorsal root ganglia for the objective quantitative assessment of neuron death after peripheral nerve injury. Exp Neurol 203:22-33.
West CA, Ljungberg C, Wiberg M, Hart A (2013) Sensory neuron death after upper limb nerve injury and protective effect of repair: clinical evaluation using volumetric magnetic resonance imaging of dorsal root Ganglia. Neurosurgery 73:632-640.
Wojcikowski K, Gobe G (2014) Animal studies on medicinal herbs: predictability, dose conversion and potential value. Phytother Res 28:22-27.
Wood MD, Gordon T, Kim H, Szynkaruk M, Phua P, Lafontaine C, Kemp SW, Shoichet MS, Borschel GH (2013) Fibrin gels containing GDNF microspheres increase axonal regeneration after delayed peripheral nerve repair. Regen Med 8:27-37.
Wood MD, Hunter D, Mackinnon SE, Sakiyama-Elbert SE (2010) Heparin-binding-affinity-based delivery systems releasing nerve growth factor enhance sciatic nerve regeneration. J Biomater Sci Polym Ed 21:771-787.
Yang CC, Wang J, Chen SC, Jan YM, Hsieh YL (2015) Enhanced functional recovery from sciatic nerve crush injury through a combined treatment of cold-water swimming and mesenchymal stem cell transplantation. Neurol Res 37:816-826.
Yang JS (2010) Treatment for cold type facial paralysis by modified Qian Zheng San together with Ginger moxibustion. Zhongyi Zazhi 7:71-74.
Yu H, Peng J, Guo Q, Zhang L, Li Z, Zhao B, Sui X, Wang Y, Xu W, Lu S (2009) Improvement of peripheral nerve regeneration in acellular nerve grafts with local release of nerve growth factor. Microsurgery 29:330-336.
Zeng W, Rong M, Hu X, Xiao W, Qi F, Huang J, Luo Z (2014) Incorporation of chitosan microspheres into collagen-chitosan scaffolds for the controlled release of nerve growth factor. PLoS One 9:e101300.
Zhang P, Zhang C, Kou Y, Yin X, Zhang H, Jiang B (2009) The histological analysis of biological conduit sleeve bridging rhesus monkey median nerve injury with small gap. Artif Cells Blood Substit Immobil Biotechnol 37:101-104.
Zhang P, Kou Y, Yin X, Wang Y, Zhang H, Jiang B (2011) The experimental research of nerve fibers compensation amplification innervation of ulnar nerve and musculocutaneous nerve in rhesus monkeys. Artif Cells Blood Substit Immobil Biotechnol 39:39-43.
Zhang P, Wang Z, Kou Y, Han N, Xu C, Yin X, Wang Y, Feng X (2014) Role of lumbricus extract in the nerve amplification effect during peripheral nerve regeneration. Am J Transl Res 6:876-885.
Zhang W, Zhou G, Gao Y, Zhou Y, Liu J, Zhang L, Long A, Zhang L, Tang P (2017) A sequential delivery system employing the synergism of EPO and NGF promotes sciatic nerve repair. Colloids Surf B Biointerfaces 159:327-336.
Zhang Y, Sun HM, He X, Wang YY, Gao YS, Wu HX, Xu H, Gong XG, Guo ZY (2013) Da-Bu-Yin-Wan and Qian-Zheng-San, two traditional Chinese herbal formulas, up-regulate the expression of mitochondrial subunit NADH dehydrogenase 1 synergistically in the mice model of Parkinson's disease. J Ethnopharmacol 146:363-371.
Zhuang H, Bu S, Hua L, Darabi MA, Cao X, Xing M (2016) Gelatin-methacrylamide gel loaded with microspheres to deliver GDNF in bilayer collagen conduit promoting sciatic nerve growth. Int J Nanomedicine 11:1383-1394.

P-Reviewer: Urbanchek MG; C-Editor: Zhao M; S-Editors: Wang J, Li CH; L-Editors: Qiu Y, Song LP; T-Editor: Liu XL